

Mobile phone jammer Welland | advantages of mobile phone jammer

[Home](#)

>

[mobile phone jammer australia](#)

>

mobile phone jammer Welland

- [advanced mobile phone signal jammer with highlow o](#)
- [advantages of mobile phone jammer](#)
- [buy mobile phone jammer](#)
- [electronic mobile phone jammer](#)
- [gps mobile phone jammer abstract judgment](#)
- [gps mobile phone jammer abstract request](#)
- [gps mobile phone jammer factory](#)
- [gps mobile phone jammer for sale](#)
- [gps mobile phone jammer laws](#)
- [how can i make a mobile phone jammer](#)
- [mini portable mobile phone signal jammer](#)
- [mobile phone jammer Manitoba](#)
- [mobile phone jammer New Brunswick](#)
- [mobile phone and gps jammer china](#)
- [mobile phone gps jammer app](#)
- [mobile phone gps jammer yakima](#)
- [mobile phone jammer australia](#)
- [mobile phone jammer circuit pdf](#)
- [mobile phone jammer cost](#)
- [mobile phone jammer dealers](#)
- [mobile phone jammer dealers in kerala](#)
- [mobile phone jammer detector](#)
- [mobile phone jammer Dieppe](#)
- [mobile phone jammer for home](#)
- [mobile phone jammer in hyderabad](#)
- [mobile phone jammer in uk](#)
- [mobile phone jammer ireland](#)
- [mobile phone jammer Kawartha Lakes](#)
- [mobile phone jammer manufacturer](#)
- [mobile phone jammer Melville](#)
- [mobile phone jammer Mercier](#)
- [mobile phone jammer Nottingham](#)
- [mobile phone jammer overview](#)
- [mobile phone jammer Penticton](#)
- [mobile phone jammer Port Colborne](#)
- [mobile phone jammer price in india](#)

- [mobile phone jammer Prince Edward County](#)
- [mobile phone jammer Prince Rupert](#)
- [mobile phone jammer Steinbach](#)
- [mobile phone jammer Thurso](#)
- [mobile phone jammer Trail](#)
- [mobile phone jammer York](#)
- [mobile phone jammers in pakistan](#)
- [mobile phone signal jammer with pre scheduled time](#)
- [mobile phone signal jammer with remote control](#)
- [mobilephonejammers](#)
- [office mobile phone jammer](#)
- [phone mobile jammer yakima](#)
- [raspberry pi mobile phone jammer](#)
- [where can i get a mobile phone jammer](#)

Permanent Link to Space-Time Equalization Techniques for New GNSS Signals
2021/04/09

By Pratibha B. Anantharamu, Daniele Borio, and Gérard Lachapelle Spatial and temporal information of signals received from multiple antennas can be applied to mitigate the impact of new GPS and Galileo signals' binary-offset sub-carrier, reducing multipath and interference effects. New modernized GNSS such as GPS, Galileo, GLONASS, and Compass broadcast signals with enhanced correlation properties as compared to the first generation GPS signals. These new signals are characterized by different modulations that provide improved time resolution, resulting in more precise range measurements, along with the advantage of being more resilient to multipath and RF interference. One of these modulations is the binary-offset-carrier (BOC) modulation transmitted by Galileo and modernized GPS. Despite the benefits of BOC modulation schemes, difficulties in tracking BOC signals can arise. The autocorrelation function (ACF) of BOC signals is multi-peaked, potentially leading to false peak-lock and ambiguous tracking. Intense research activities have produced different BOC tracking schemes that address the issue of multi-peaked BOC signal tracking. Additionally, new tracking schemes including space-time processing can be adopted to further improve the performance of existing algorithms. Space-time equalization is a technique that utilizes spatial and temporal information of signals received from multiple antennas to compensate for the effects of multipath fading and co-channel interference. In the context of BOC signals, these kinds of techniques can be applied to mitigate the impact of the sub-carrier, which is responsible for a multi-peaked ACF, reducing multipath and interference effects. In temporal processing, traditional equalizers in time-domain are useful to compensate for signal distortions. But equalization becomes more challenging in the case of BOC signals, where the effect of both sub-carrier and multipath must be accounted for. On the other hand, by using spatial processing, it should be possible to extract the desired signal component from a set of received signals by electronically varying the antenna array directivity (beamforming). The combination of an antenna array and a temporal equalizer results in better system performance. Hence the main objective of this research is to apply space-time processing techniques to BOC modulated signals received by an antenna array. The main intent is to enhance the signal quality, avoid

ambiguous tracking and improve tracking performance under weak signal environments or in the presence of harsh multipath components. The focus of previous antenna-array processing using GNSS signals was on enhancing GNSS signal quality and mitigating interference and/or multipath related issues. Unambiguous tracking was not considered. Here, we develop a space-time algorithm to mitigate ambiguous tracking of BOC signals along with improved signal quality. The main objective is to obtain an equalization technique that can operate on BOC signals to provide unambiguous BPSK-like correlation function capable of altering the antenna array beam pattern to improve the signal to interference plus noise ratio. Space-time adaptive processing structure proposed for BOC signal tracking; the temporal filter provides signal with unambiguous ACF whereas the spatial filter provides enhanced performance with respect to multipath, interference, and noise. Initially, temporal equalization based on the minimum mean square error (MMSE) technique is considered to obtain unambiguous ACF on individual antenna outputs. Spatial processing is then applied on the correlator outputs based on a modified minimum variance distortionless response (MVDR) approach. As part of spatial processing, online calibration of the real antenna array is performed which also provides signal and noise information for the computation of the beamforming weights. Finally, the signal resulting from temporal and spatial equalization is fed to a common code and carrier tracking loop for further processing. The effectiveness of the proposed technique is demonstrated by simulating different antenna array structures for BOC signals. Intermediate-frequency (IF) simulations have been performed and linear/planar array structures along with different signal to interference plus noise ratios have been considered. A modified version of The University of Calgary software receiver, GSNRx, has been used to simultaneously process multi-antenna data. Further tests have been performed using real data collected from Galileo test satellites, GIOVE-A and GIOVE-B, using an array structure comprising of two to four antennas. A 4-channel front-end designed in the PLAN group, and a National Instruments (NI) signal vector analyzer equipped with three PXI-5661 front-ends (NI 2006) have been used to collect data synchronously from several antennas. The data collected from the antennas were progressively attenuated for the analysis of the proposed algorithm in weak signal environments. From the performed tests and analysis, it is observed that the proposed methodology provides unambiguous ACF. Spatial processing is able to efficiently estimate the calibration parameters and steer the antenna array beam towards the direction of arrival of the desired signal. Thus, the proposed methodology can be used for efficient space-time processing of new BOC modulated GNSS signals.

Signal and Systems Model The complex baseband GNSS signal vector received at the input of an antenna array can be modeled as (1) where

- M is the number of antenna elements;
- L is the number of satellites;
- C is a $M \times M$ calibration matrix capturing the effects of antenna gain/phase mismatch and mutual coupling;
- $s_i =$ is the complex $M \times 1$ steering vector relative to the signal from the i th satellite. s_i captures the phase offsets between signals from different antennas;
- n is the noise plus interference vector observed by the M antennas. The i th useful signal component $x_i(t)$ can be modeled as (2) where
- A_i is the received signal amplitude;
- $d_i()$ models the navigation data bit;
- $c_i()$ is the ranging sequence used for spreading the transmitted data;
- $\tau_{0,i}$, $f_{0,i}$ and $\phi_{0,i}$ model the code delay,

Doppler frequency and carrier phase introduced by the communication channel. The index i is used to denote quantities relative to the i th satellite. The ranging code $c_i()$ is made up of several components including a primary spreading sequence, a secondary code and a sub-carrier. For a BPSK modulated signal, the sub-carrier is a rectangular window of duration T_c . In the case of BOC modulated signals, the sub-carrier is generated as the sign of a sinusoidal carrier. The presence of this sub-carrier produces a multi-peaked autocorrelation function making the acquisition/tracking processes ambiguous. In order to extract signal parameters such as code delay and Doppler frequency of the i th useful signal $x_i(t)$, the incoming signal is correlated with a locally generated replica of the incoming code and carrier. This process is referred to as correlation where the carrier of the incoming signal is at first wiped off using a local complex carrier replica. The spreading code is also wiped off using a ranging code generator. The signal obtained after carrier and code removal is integrated and dumped over T seconds to provide correlator outputs. The correlator output for the h th satellite and m th antenna can be modeled as: (3) where $v_{m,k}$ are the coefficients of the calibration matrix, C and $R(\Delta\tau_h)$ is the multi-peaked ACF. τ_h , $f_{D,h}$ and ϕ_h are the code delay, Doppler frequency and carrier phase estimated by the receiver and $\Delta\tau_h$, $\Delta f_{D,h}$ and $\Delta\phi_h$ are the residual delay, frequency, and phase errors. η is the residual noise term obtained from the processing of $\eta(t)$. Eq. (3) is the basic signal model that will be used for the development of a space-time technique suitable for unambiguous BOC tracking. When BOC signals are considered, algorithms should be developed to reduce the impact of that include receiver noise, interference and multipath components, along with the mitigation of ambiguities in $R(\Delta\tau_h)$. Space-time processing techniques have the potential to fulfill those requirements. Space-Time Processing A simplified representation of a typical space-time processing structure is provided in Figure 1. Each antenna element is followed by K taps with δ denoting the time delay between successive taps forming the temporal filter. The combination of several antennas forms the spatial filter. $w_{m,k}$ are the space-time weights with $0 \leq k \leq K$ and $0 \leq m \leq M$. k is the temporal index and m is the antenna index. Figure 1. Block diagram of space-time processing. The array output after applying the space-time filter can be expressed as (4) where $(w_{m,k})^*$ denotes complex conjugate. The spatial-only filter can be realized by setting $K=1$ and a temporal only filter is obtained when $M=1$. The weights are updated depending on the signal/channel characteristics subject to user-defined constraints using different adaptive techniques. This kind of processing is often referred to as Space-Time Adaptive Processing (STAP). The success of STAP techniques has been well demonstrated in radar, airborne and mobile communication systems. This has led to the application of STAP techniques in the field of GNSS signal processing. Several STAP techniques have been developed for improving the performance of GNSS signal processing. These techniques exploit the advantages of STAP to minimize the effect of multipath and interference along with improving the overall signal quality. Space-time processing algorithms can be broadly classified into two categories: decoupled and joint space-time processing. The joint space-time approach exploits both spatial and temporal characteristics of the incoming signal in a single space-time filter while the decoupled approach involves several temporal equalizers and a spatial beamformer that are realized in two separate stages (Figure 2). Figure 2. Representation of two different space-time processing techniques When considering


the decoupled approach for GNSS signals, temporal filters can be applied on the data from the different antennas whereas the spatial filter can be applied at two different stages, namely pre-correlation or post-correlation. In the pre-correlation stage, spatial weights are applied on the incoming signal after carrier wipe-off while in the post-correlation stage, spatial weights are applied after the Integrate & Dump (I&D) block on the correlator outputs. In pre-correlation processing, the update rate of the weight vector is in the order of MHz (same as the sampling frequency) whereas the post-correlation processing has the advantage of lower update rates in the order of kHz (I&D frequency). In the pre-correlation case, the interference and noise components prevail significantly in the spatial correlation matrix and would result in efficient interference mitigation and noise reduction. But the information on direct and reflected signals are unavailable since the GNSS signals are well below the noise level. This information can be extracted using post-correlation processing. In the context of new GNSS signals, efforts to utilize multi-antenna array to enhance signal quality along with interference and multipath mitigation have been documented using both joint and decoupled approaches where the problem of ambiguous signal tracking was not considered. In our research, we considered the decoupled space-time processing structure. Temporal processing is applied at each antenna output and spatial processing is applied at the post-correlation stage. Temporal processing based on MMSE equalization and spatial processing based on the adaptive MVDR beamformer are considered. Methodology The opening figure shows the proposed STAP architecture for BOC signal tracking. In this approach, the incoming BOC signals are at first processed using a temporal equalizer that produces a signal with a BPSK-like spectrum. The filtered spectra from several antennas are then combined using a spatial beamformer that produces maximum gain at the desired signal direction of arrival. The beamformed signal is then fed to the code and carrier lock loops for further processing. The transfer function of the temporal filter is obtained by minimizing the error: (5) where $H(f)$ is the transfer function of the temporal filter that minimizes the MSE, ϵ_{MMSES} , between the desired spectrum, $G_D(f)$, and filtered spectrum, $G_x(f)H(f)$. The spectrum of the incoming BOC signal is denoted by $G_x(f)$. λ is a weighting factor determining the impact of noise with respect to that of an ambiguous correlation function. N_0 is the noise power spectral density and C the carrier power. The desired spectrum is considered to be a BPSK spectrum. Since this type of processing minimizes the MSE, it is denoted MMSE Shaping (MMSES). Figure 3 shows a sample plot of the ACF obtained after applying MMSES on live Galileo BOCs(1,1) signals collected from the GIOVE-B satellite. The input C/N_0 was equal to 40 dB-Hz and the ACF was averaged over 1 second of data. It can be observed that the multi-peaked ACF was successfully modified by MMSES to produce a BPSK-like ACF without secondary peaks. Also narrow ACF were obtained by modifying the filter design for improved multipath mitigation. Thus using temporal processing, the antenna array data are devoid of ambiguity due to the presence of the sub-carrier. After temporal equalization, the spatial weights are computed and updated based on the following information: The signal and noise covariance matrix obtained from the correlator outputs; Calibration parameters estimated to minimize the effect of mutual coupling and antenna gain/phase mismatch; Satellite data decoded from the ephemeris/almanac containing information on the GNSS signal DoA. The weights are updated using the iterative approach for the MVDR

beamformer to maximize the signal quality according to the following steps: Step 1: Update the estimate of the steering vector for the h th satellite using the calibration parameters as: (6) Here $v_{i,j}$ represents the estimated calibration parameters using the correlator outputs given by Eq. (3) and $s_{m,h}$ is the element of the steering vector computed using the satellite ephemeris/almanac data. Step 2: Update the weight vector (the temporal index, k , is removed for ease of notation) using the new estimate of the covariance matrix and steering vector as (7) where $s_{m,h}$ is the input signal after carrier wipe-off. Repeat Steps 1 and 2 until the weights converge. Finally compute the correlator output to drive the code and carrier tracking loop according to Equation (4). The C/N0 gain obtained after performing calibration and beamforming on a two-antenna linear array and four-antenna planar array data collected using the four channel front-end is provided in Figure 4 and Figure 5. The C/N0 plots are characterized by three regions: Single Antenna that provides C/N0 estimates obtained using $q_{0,h}$ alone; Before Calibration that provides C/N0 estimates obtained by compensating only the effects of the steering vector, s_i , before combining the correlator outputs from all antennas; After Calibration that provides C/N0 estimates obtained by compensating the effects of both steering vector, s_i and calibration matrix, C , before combining correlator outputs from all antennas. After calibration, beamforming provides approximately a C/N0 gain equal to the theoretical one on most of the satellites whereas before calibration, the gain is minimal and, in some cases, negative with respect to the single antenna case. These results support the effectiveness of the adopted calibration algorithm and the proposed methodology that enables efficient beamforming. Figure 4. C/N0 estimates obtained after performing calibration and beamforming on linear array data. Figure 5. C/N0 estimates obtained after performing calibration and beamforming on the planar array data. Results and Analysis IF simulated BOCs(1,1) signals for a 4-element planar array with array spacing equal to half the wavelength of the incoming signal has been considered to analyze the proposed algorithm. The input signal was characterized by a C/N0 equal to 42 dB-Hz at an angle of arrival of 20° elevation and 315° azimuth angle. A sample plot of the antenna array pattern using the spatial beamformer is shown in Figure 6. In the upper part of Figure 6, the ideal case in the absence of interference was considered. The algorithm is able to place a maximum of the array factor in correspondence of the signal DoA. Figure 6. Antenna array pattern for a 4-element planar array computed using a MVDR beamformer in the presence of two interference sources. In the bottom part, results in the presence of interference are shown. Two interference signals were introduced at 60 and 45 degree elevation angles. It can be clearly observed that, in the presence of interference, the MVDR beamformer successfully adapted the array beam pattern to place nulls in the interference DoA. In order to further test the tracking capabilities of the full system, semi-analytic simulations were performed for the analysis of digital tracking loops. The simulation scheme is shown in Figure 7 and consists of M antenna elements. Each antenna input for the h th satellite is defined by a code delay ($\tau_{m,h}$) and a carrier phase value ($\phi_{m,h}$) for DLL and PLL analysis. $\phi_{m,h}$ captures the effect of mutual coupling, antenna phase mismatch and phase effects due to different antenna hardware paths. To analyze the post-correlation processing structure, each antenna input is processed independently to obtain the error signal, $\Delta\tau_{m,h} / \Delta\phi_{m,h}$ as where $\tau_{m,h}$ and $\phi_{m,h}$ are the current delay/phase estimates. Figure 7. Semi-analytic simulation

model for a multi-antenna system comprising M antennas with a spatial beamformer. Each error signal is then used to obtain the signal components that are added along with the independent noise components, n . The combined signal and noise components from all antenna elements are fed to the spatial beamformer to produce a single output according to the algorithm described in the Methodology section. Finally, the beamformer output is passed through the loop discriminator, filter and NCO to provide a new estimate $\hat{\theta}$. The Error to Signal mapping block and the noise generation process accounts for the impact of temporal filtering. Figure 8 shows sample tracking jitter plots for a PLL with a single, dual and three-antenna array system obtained using the structure described above. Figure 8. Phase-tracking jitter obtained for single, dual and three-antenna linear array as a function of the input C/N0 for a Costas discriminator (20 milliseconds coherent integration and 5-Hz bandwidth). The number of simulation runs considered was 50000 with a coherent integration time of 20 ms and a PLL bandwidth equal to 5 Hz. As expected the tracking jitter improves when the number of antenna elements is increased along with improved tracking sensitivity. As expected, the C/N0 values at which loss of lock occurs for a three antenna system is reduced with respect to the single antenna system, showing its superiority. Real data analysis. Figure 9 shows the experimental setup considered for analysis of the proposed combined space-time algorithm. Two antennas spaced 8.48 centimeters apart were used to form a 2-element linear antenna array structure. The NI front-end was employed for the data collection process to synchronously collect data from the two-antenna system. Data on both channels were progressively attenuated by 1 dB every 10 seconds to simulate a weak signal environment until an attenuation of 20 dB was reached. When this level of attenuation was reached, the data were attenuated by 1 dB every 20 seconds to allow for longer processing under weak signal conditions. In this way, data on both antennas were attenuated simultaneously. Data from Antenna 1 were passed through a splitter, as shown in Figure 9, before being attenuated in order to collect signals used to produce reference code delay and carrier Doppler frequencies. Figure 9. Experimental setup with signals collected using two antennas spaced 8.48 centimeters apart. BOCs(1,1) signals collected using Figure 9 were tracked using the temporal and spatial processing technique described in the opening figure. The C/N0 results obtained using single and two antennas are provided in Figure 10. In the single antenna case, only temporal processing was used. In this case, the loop was able to track signals for an approximate C/N0 of 19 dB-Hz. Using the space-time processing, the dual antenna system was able to track for nearly 40 seconds longer than the single antenna case, thus providing around 2 dB improvement in tracking sensitivity. Figure 10. C/N0 estimates obtained using a single antenna, temporal only processing and a dual-antenna array system using space-time processing. Conclusions A combined space-time technique for the processing of new GNSS signals including a temporal filter at the output of each antenna, a calibration algorithm and a spatial beamformer has been developed. The proposed methodology has been tested with simulations and real data. It was observed that the proposed methodology was able to provide unambiguous tracking after applying the temporal filter and enhance the signal quality after applying a spatial beamformer. The effectiveness of the proposed algorithm to provide maximum signal gain in the presence of several interference sources was shown using simulated data. C/N0 analysis for real data collected using

a dual antenna array showed the effectiveness of combined space-time processing in attenuated signal environments providing a 2 dB improvement in tracking sensitivity. Pratibha B. Anantharamu received her doctoral degree from Department of Geomatics Engineering, University of Calgary, Canada. She is a senior systems engineer at Accord Software & Systems Pvt. Ltd., India. □Daniele Borio received a doctoral degree in electrical engineering from Politecnico di Torino. He is a post-doctoral fellow at the Joint Research Centre of the European Commission.□ Gérard Lachapelle holds a Canada Research Chair in Wireless Location in the Department of Geomatics Engineering, University of Calgary, where he heads the Position, Location, and Navigation (PLAN) Group.

mobile phone jammer Welland

Auto no break power supply control.hand-held transmitters with a „rolling code“ can not be copied,as many engineering students are searching for the best electrical projects from the 2nd year and 3rd year,many businesses such as theaters and restaurants are trying to change the laws in order to give their patrons better experience instead of being consistently interrupted by cell phone ring tones.5 kgadvanced modelhigher output powersmall sizecovers multiple frequency band.5% to 90%modeling of the three-phase induction motor using simulink.a frequency counter is proposed which uses two counters and two timers and a timer ic to produce clock signals, ,frequency counters measure the frequency of a signal.three circuits were shown here,2 ghzparalyses all types of remote-controlled bombshigh rf transmission power 400 w,this paper describes the simulation model of a three-phase induction motor using matlab simulink.50/60 hz permanent operationtotal output power,where shall the system be used,commercial 9 v block batterythe pki 6400 eod convoy jammer is a broadband barrage type jamming system designed for vip.this circuit shows a simple on and off switch using the ne555 timer.this paper shows the controlling of electrical devices from an android phone using an app,scada for remote industrial plant operation,preventively placed or rapidly mounted in the operational area.2100 - 2200 mhz 3 gpower supply,the first types are usually smaller devices that block the signals coming from cell phone towers to individual cell phones,exact coverage control furthermore is enhanced through the unique feature of the jammer.ix conclusionthis is mainly intended to prevent the usage of mobile phones in places inside its coverage without interfacing with the communication channels outside its range.they are based on a so-called „rolling code“,6 different bands (with 2 additinal bands in option)modular protection.the data acquired is displayed on the pc.transmission of data using power line carrier communication system.by activating the pki 6050 jammer any incoming calls will be blocked and calls in progress will be cut off.the components of this system are extremely accurately calibrated so that it is principally possible to exclude individual channels from jamming.the pki 6200 features achieve active stripping filters,with an effective jamming radius of approximately 10 meters,the integrated working status indicator gives full information about each band module.it has the power-line data communication circuit and uses ac power line to send operational status and to receive necessary control signals.when zener diodes are operated in reverse bias at a particular voltage level,1800 mhzparalyses all kind of cellular and portable phones1 w output

powerwireless hand-held transmitters are available for the most different applications,when the brake is applied green led starts glowing and the piezo buzzer rings for a while if the brake is in good condition,go through the paper for more information,from analysis of the frequency range via useful signal analysis.this paper describes different methods for detecting the defects in railway tracks and methods for maintaining the track are also proposed,- active and passive receiving antennaoperating modes,a constantly changing so-called next code is transmitted from the transmitter to the receiver for verification,3 w output powergsm 935 - 960 mhz,all mobile phones will automatically re-establish communications and provide full service,while the second one is the presence of anyone in the room.energy is transferred from the transmitter to the receiver using the mutual inductance principle.the jamming frequency to be selected as well as the type of jamming is controlled in a fully automated way.

| | |
|--|------|
| advantages of mobile phone jammer | 1780 |
| mobile phone & wifi signal jammers | 5612 |
| mobile phone and gps jammer iran | 3950 |
| mobile phone jammer Flin Flon | 1352 |
| gps and mobile phone signal jammer | 2480 |
| mobile phone jammer range | 6687 |
| gsm mobile jammer headphones | 5002 |
| phone mobile jammer lammy | 6345 |
| mobile phone jammer maplin | 3630 |
| mobile phone jammer Airdrie | 5563 |
| mobile phone jammer Bedford | 7046 |
| raspberry pi mobile phone jammer | 2720 |
| gps mobile phone jammer abstract driving | 2160 |
| phone mobile jammer on the market | 4884 |
| circuit of mobile phone jammer | 4322 |
| build a mobile phone jammer | 8556 |
| how to build a mobile phone jammer | 6618 |
| mobile phone jammer ppt free download | 2498 |
| mobile phone jammer Brossard | 6507 |
| mini handheld mobile phone and gps signal jammer | 2548 |
| mobile phone jammer La Malbaie | 7113 |
| mobile phone jammer Fort St. John | 3769 |
| cell phone mobile jammer idea application | 6583 |

Vehicle unit 25 x 25 x 5 cmoperating voltage.but are used in places where a phone call would be particularly disruptive like temples.-10°c - +60°crelative humidity,jammer disrupting the communication between the phone and the cell phone base station in the tower.because in 3 phases if there any phase reversal it

may damage the device completely. it should be noted that these cell phone jammers were conceived for military use. at every frequency band the user can select the required output power between 3 and 1, this system also records the message if the user wants to leave any message, the light intensity of the room is measured by the ldr sensor. that is it continuously supplies power to the load through different sources like mains or inverter or generator. this system is able to operate in a jamming signal to communication link signal environment of 25 db, the second type of cell phone jammer is usually much larger in size and more powerful, i have designed two mobile jammer circuits, railway security system based on wireless sensor networks, but with the highest possible output power related to the small dimensions. according to the cellular telecommunications and internet association. this paper shows a converter that converts the single-phase supply into a three-phase supply using thyristors, this article shows the circuits for converting small voltage to higher voltage that is 6v dc to 12v but with a lower current rating. it could be due to fading along the wireless channel and it could be due to high interference which creates a dead-zone in such a region. law-courts and banks or government and military areas where usually a high level of cellular base station signals is emitted. one is the light intensity of the room. this project shows the controlling of bldc motor using a microcontroller. the marx principle used in this project can generate the pulse in the range of kv, a blackberry phone was used as the target mobile station for the jammer. the circuit shown here gives an early warning if the brake of the vehicle fails, bomb threats or when military action is underway. that is it continuously supplies power to the load through different sources like mains or inverter or generator, the scope of this paper is to implement data communication using existing power lines in the vicinity with the help of x10 modules, its total output power is 400 w rms. my mobile phone was able to capture majority of the signals as it is displaying full bars. v test equipment and proceduredigital oscilloscope capable of analyzing signals up to 30mhz was used to measure and analyze output wave forms at the intermediate frequency unit, it detects the transmission signals of four different bandwidths simultaneously, this project shows the generation of high dc voltage from the cockcroft -walton multiplier, -20°c to +60°c ambient humidity, 0°c - +60°c relative humidity, the zener diode avalanche serves the noise requirement when jammer is used in an extremely silet environment, the inputs given to this are the power source and load torque, in case of failure of power supply alternative methods were used such as generators. solar energy measurement using pic microcontroller. 2110 to 2170 mhz total output power. the rft comprises an in build voltage controlled oscillator, when the mobile jammers are turned off, this project shows the starting of an induction motor using scr firing and triggering. this is also required for the correct operation of the mobile. we hope this list of electrical mini project ideas is more helpful for many engineering students, variable power supply circuits.

By this wide band jamming the car will remain unlocked so that governmental authorities can enter and inspect its interior. frequency correction channel (fcch) which is used to allow an ms to accurately tune to a bs. the multi meter was capable of performing continuity test on the circuit board. it is specially customised to accommodate a broad band bomb jamming system covering the full spectrum from 10 mhz to 1, we have already published a list of electrical projects which are collected

from different sources for the convenience of engineering students, today's vehicles are also provided with immobilizers integrated into the keys presenting another security system, the common factors that affect cellular reception include, protection of sensitive areas and facilities. 1 watt each for the selected frequencies of 800, pulses generated in dependence on the signal to be jammed or pseudo generated manually via audio in, its built-in directional antenna provides optimal installation at local conditions. phs and 3g the pki 6150 is the big brother of the pki 6140 with the same features but with considerably increased output power. auto no break power supply control, high efficiency matching units and omnidirectional antenna for each of the three bands total output power 400 w rms cooling. this system does not try to suppress communication on a broad band with much power. smoke detector alarm circuit. noise circuit was tested while the laboratory fan was operational, a prerequisite is a properly working original hand-held transmitter so that duplication from the original is possible. it is required for the correct operation of radio system. mobile jammer was originally developed for law enforcement and the military to interrupt communications by criminals and terrorists to foil the use of certain remotely detonated explosive. this paper shows a converter that converts the single-phase supply into a three-phase supply using thyristors, this causes enough interference with the communication between mobile phones and communicating towers to render the phones unusable, this task is much more complex. the operating range is optimised by the used technology and provides for maximum jamming efficiency. 1800 to 1950 mhz on dcs/phs bands. a user-friendly software assumes the entire control of the jammer. the proposed system is capable of answering the calls through a pre-recorded voice message. the rf cellular transmitter module with 0, zigbee based wireless sensor network for sewerage monitoring. different versions of this system are available according to the customer's requirements, sos or searching for service and all phones within the effective radius are silenced, is used for radio-based vehicle opening systems or entry control systems, a mobile jammer circuit or a cell phone jammer circuit is an instrument or device that can prevent the reception of signals by mobile phones, this device is the perfect solution for large areas like big government buildings, upon activating mobile jammers, the circuit shown here gives an early warning if the brake of the vehicle fails, the aim of this project is to achieve finish network disruption on gsm- 900mhz and dcs-1800mhz downlink by employing extrinsic noise, the cockcroft walton multiplier can provide high dc voltage from low input dc voltage. you may write your comments and new project ideas also by visiting our contact us page. cell phones within this range simply show no signal. cell phone jammers have both benign and malicious uses, micro controller based ac power controller. the jammer is portable and therefore a reliable companion for outdoor use, an indication of the location including a short description of the topography is required. this paper shows the controlling of electrical devices from an android phone using an app, if there is any fault in the brake red led glows and the buzzer does not produce any sound.

Overload protection of transformer, this project uses arduino for controlling the devices. ac power control using mosfet / igbt. once i turned on the circuit, it should be noted that operating or even owning a cell phone jammer is illegal in most municipalities and specifically so in the united states, a piezo sensor is used for touch

sensing, the device looks like a loudspeaker so that it can be installed unobtrusively. please see the details in this catalogue..

- [mobile phone jammer Weyburn](#)
- [define :mobile phone jammer](#)
- [mobile phone jammer Brockville](#)
- [mobile phone jammer circuit diagram pdf](#)
- [mobile phone jammer Summerside](#)
- [advanced mobile phone signal jammer with highlow o](#)
- [advanced mobile phone signal jammer with highlow o](#)
- [advanced mobile phone signal jammer with highlow o](#)
- [advanced mobile phone signal jammer with highlow o](#)
- [advanced mobile phone signal jammer with highlow o](#)

- [mobile phone jammer circuit diagram](#)
- [rx10 handheld mobile phone jammer photo](#)
- [jammer mobile phone tools](#)
- [mobile phone jammer Burnaby](#)
- [mobile phone jammer Gracefield](#)
- [advanced mobile phone signal jammer with highlow o](#)
- [advanced mobile phone signal jammer with highlow o](#)
- [advanced mobile phone signal jammer with highlow o](#)
- [mobile phone jammer manufacturer](#)
- [mobile phone jammer manufacturer](#)

- [Signal Jamming](#)

- [kifinale.de](#)

Email:L5_tOI9@gmail.com

2021-04-08

Sony svt11 svf13n 44w 19.5v 2.5a ac adapter.41-12-300 d ac adapter 12vdc 300ma used -(+) 1x3.5mm round barre.new original 12v 800ma homedics ma411208 ac adapter,adp da-24b12-c ac adapter 12v 2a da24b12c,friwo d-6980 ac adapter 2.4vdc used -(+) 1.7x4.9mm straight roun.new 4.5v 400ma magnavox ay 3160/17 power supply ac adapter,konica minolta ac-4 ac adapter 4.7vdc 2a switching power supply..

Email:b0acl_XO7Rb9v@aol.com

2021-04-06

New pace 2901-800058-002 eadp-36fb ac adapter 12v 3a power supply.new 12v 500ma radioshack ad-316 ac adapter,acer aspire 1680 1690 3000 5000 3630 3640 cpu cooling fan 36zl2t,fonegear 05011 retractabile travel charger 4.4-5vdc 400ma.new philips ay3170/17 4.5v dc 300ma ac adapter cd player power supply,fincom 1000-500031-000 ac adapter 5.1vdc 2.2a replacement switc,fuji fujifilm genuine original ac-5vhs-us ac adapter 5v 1.5a for ac-5vw ac-5v ac-5vs finepix 2400 6900 6800 s7000 mx-290..

Email:T9qN_Qd1LN@aol.com

2021-04-03

Oh-57079dt ac adapter 12vdc 2000ma used -(+) 2pin 2pin din medic.new ault mw116 ka1249f04 power supply 12v 6.67a ac adpater 4pin,ibm 40y7698 93p5026 laptop ac adapter with cord/charger.mkd-350600350 ac adapter 6vdc 350ma used 2x5.5x11mm -(+)-.mode dv-1280-3 ac adapter 12vdc 1a class 2 transformer wallmount,.

Email:yvAE_ZDYJbqgh@yahoo.com

2021-04-03

Ul listed 12v dc 1amp power supply switch adapter transformer chargers this auction is for one lot of 100 piec.xata sa-0022-02 automatic fuses,dell pa-3 ac adapter 19vdc 2.4a 2.5x5.5mm -(+) power supply,original 12vac 2.5a triad magnetics wau12-2500 wall mount adapter power supply,lenovo5a10g68679 20v 3.25a 65w replacement ac adapter..

Email:MoEuN_VEY65wO@gmail.com

2021-03-31

Digipower acd-nk25 110-220v ac dc adapter switching power supply.apd 12v 3a asian power devices da-36v12 ac adapter 5.5/2.5mm da-36v12 products specifications model da-36v12 item con,oem aa-1283 ac adapter 12vac 830ma ~(~)~ 2x5.5mm used 90° 2 x 5..6v cigar auto car charger car adapter for eton radio s350dl s350dl-r.radio battery charger base & adapter for motorola walkie talkie gp328 ht1250 etc compatible product: walkie talkie co,ibm/lenovo t500 w500 integrat heatsink fan 45n5490,globtek gt-21097-5024 ac adapter 24vdc 2.1a ite power supply 3pi,.